Analysing Growth in Faces

R. J. Morris
Department of Statistics
University of Leeds
Leeds, England

J. T. Kent
Department of Statistics
University of Leeds
Leeds, England

K. V. Mardia
Department of Statistics
University of Leeds
Leeds, England

M. Fidrich
Department of Informatics
Jozsef Attila University
Hungary

R. G. Aykroyd
Department of Statistics
University of Leeds
Leeds, England

A. Linney
Medical Physics Group
University College London
London, England

Abstract ***We examine the changes in the profile of the human face with age. First the medial plane running down the middle of the face is found using a variant of the Iterative Closest Point Algorithm, optimising over the set of reflections. The boundary of the silhouette as viewed from the side is extracted. Landmarks are found using bitangent lines and extremals of distance. A representation of size and shape is found using Procrustes Analysis. Principal Component Analysis is used to examine how size and shape varies with growth. Promising early results are presented.***

Keywords: Shape Analysis, Facial Growth, Registration, Iterative Closest Point Algorithm, Procrustes Analysis

1 Introduction

In this paper we will discuss a semi-automatic method for analysing growth of faces and present some preliminary results. We will concentrate on landmarks lying on the medial plane which separates the left and right sides of the face. The general scheme we will follow is: find the plane of symmetry (Section 2); extract the profile (§3); find a set of homologous landmarks (§4); use Procrustes Analysis and Principal Component Analysis to analyse the size and shape information (§5).

We have obtained a set of laser scans [12] from a number of individuals with between two and eight scans per subject taken at ages between 5 and 15. Each scan consists of about 30,000 3D points arranged as a mesh of quadrilaterals. For the purpose of this paper we do a preliminary analysis of the scans of five individuals (a total of 28 scans in all).

The study of the human face presents a number of challenges to shape analysis due to the wide variation in shape between subjects and the fact that different parts grow at different rates. Furthermore, finding landmarks on the face is a non trivial process, and the anatomical landmarks are not always suitable for computer-based visualisation systems.

The face has been well-studied by anatomists, and there is a vast literature on the subject. Of particular interest are the following. Enlow and Hans [4, Ch. 8] which describes the major types of head forms and patterns of growth. Farkas and colleagues have written a series of articles [5] describing how the mean distance between landmarks changes with age. Feik and Glover [6] review some of the major findings about growth of the head. For children between 5 and 15, these works conclude that there is considerable growth in the nose, less growth in the jaw, and very little in the lips and forehead. We will examine how well these conclusions are supported by our results.

The statistical analysis of faces dates back to Galton. In his earlier work [7] he looked at variations in the positions of various landmarks with respect to a fixed base line. His later work [8] classified segments between landmarks of a profile according to a number of prototypes. Much work has also been done in the statistical analysis of shape. A detailed introduction to the subject can be found in [3].

2 Finding the Medial Plane

In this section we describe a method for finding the *medial plane* of a head. This is the plane which runs vertically down through the nose separating the left and right sides of the head. We use a version of the Iterative Closest Point algorithm (ICP) to find a sequence of planes each of which is a closer approximation to the medial plane. See [1] for a discussion of the ICP algorithm. Our algorithm is similar to the "Head-in-the-Hat" algorithm of Pelizzari and Chen [13].

Let $X = \{\mathbf{x}_i \in \mathbf{R}^3 : 1 \leq i \leq n\}$ be a set of points representing the head, with $n \approx 30,000$. Given a plane P let $\mathcal{R}_P$ denote the reflection in P. The ICP algorithm consists of a number of steps:

1. Choose an initial plane P by hand.

2. For each $\mathbf{x}_i \in X$ define $\mathbf{y}_i \in X$ to be the closest point in X to $\mathcal{R}_P(\mathbf{x}_i)$.

3. Let $d_i = \|\mathbf{x}_i - \mathbf{y}_i\|$. Let $w_i = 1$ if $d_i < d$, $w_i = 0$ otherwise. Thus d_i is approximately twice the distance from x_i to P, and d is chosen to be twice the width of the nose. If either $\mathbf{x}_i$ or $\mathbf{y}_i$ lies on the boundary of the polygonization of the head then w_i is also set to zero.

4. Find the plane Q which minimises

$$\frac{1}{\sum w_i} \sum_{i=1}^{n} w_i \left|\mathbf{x}_i - \mathcal{R}_Q(\mathbf{y}_i)\right|^2 ,$$

over Q.

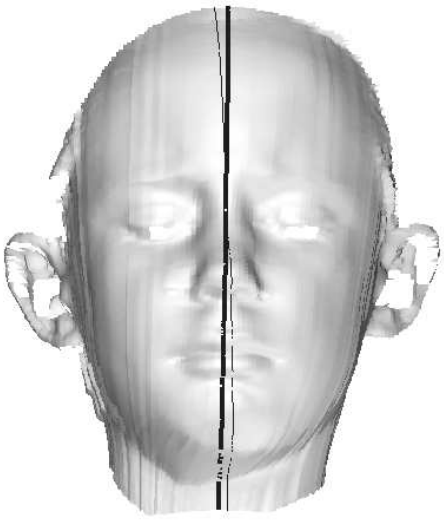

Figure 1: The initial hand estimate of the medial plane (thin line), and the final estimate after ICP (thicker line).

5. Set $P = Q$ and repeat steps 2-5 until convergence.

In practice steps 2-5 are repeated thirty times. This gave a good convergence on all the subjects tested.

The slowest part of the algorithm is step 2 which finds the closest points X for each point in $\mathcal{R}_P(\mathbf{x}_i)$. A simple minded approach calculates the distance to every point in the set. As we have about 30,000 points for each face, this can take a considerable time. This step can be speeded up by about ninety-fold by using a geometric hash table consisting of a $7 \times 7 \times 7$ array of boxes. Most of the time we just need to to check the distances to points lying inside just one of these boxes.

One side of the head is normally slightly larger than the other so using an unweighted sum in step 4 would result in a medial plane which is shifted a little to one side. Using the weighting function in step 3 largely eliminates this problem. Testing for points on the boundary eliminates problems when there are holes in the data.

A least squares technique is used to minimise the sum in step 4. We follow the work Mardia et. al. [11] who look at the equivalent prob-

lem of reflections in planes through the origin. Write the plane Q as $ax + by + cz = d$ with $\mathbf{a} = (a, b, c)^T$ a unit length vector. The reflection of a point $\mathbf{x}$ is $\mathcal{R}_Q(\mathbf{x}) = \mathbf{x} + 2(d - \mathbf{a}^T\mathbf{x})\mathbf{a}$. The sum in step 4 is minimised when $\mathbf{a}$ is the solution of the eigenvalue problem $(C - \mathbf{m}\mathbf{m}^T)\mathbf{a} = \lambda\mathbf{a}$ with minimum eigenvalue and $d = \frac{1}{2}\mathbf{m}^T\mathbf{a}$. Here C is the covariance-like matrix $\sum_i w_i(\mathbf{x}_i\mathbf{y}_i^T + \mathbf{y}_i\mathbf{x}_i^T)/(2\sum_i w_i)$ and $\mathbf{m} = \sum_i(w_i\mathbf{x}_i + \mathbf{y}_i)/(2\sum_i w_i)$.

Figure 1 shows the results of the ICP algorithm. The thin line is our original hand estimate of the medial plane and the thicker line is the estimate after ten iterations. The hand-estimate was chosen poorly to illustrate the benificial effects of the algorithm; we can see that the final result is much closer to what we expect the medial plane to be.

3 Calculating Profiles

We now simplify the problem to a two dimensional one by calculating the profile of the surface as seen from the right-hand side of the head.

Each head is first rotated into a standard coordinate system with $z = 0$ being the medial plane and the z-axis running out through the right ear. For convenience we also rotate the head around the z-axis so that the x-axis runs out through the nose and the y-axis runs through the top of the head.

We now want to extract the profile seen when looking along the z-axis. There are two natural ways this profile can can be defined and extracted:

1. calculate the intersection of the head with $z = 0$ (intersection profile);
2. calculate the boundary of the shadow cast by light rays parallel to the z-axis onto a plane parallel to $z = 0$ lying entirely behind the surface (shadow boundary or silhouette boundary).

If the head is perfectly symmetrical about $z = 0$, then both methods will give the same results. However the second method is generally less sensitive to errors in selecting the medial plane. In particular translating the head along the z-axis does not change the shadow boundary. We use the second method in this paper.

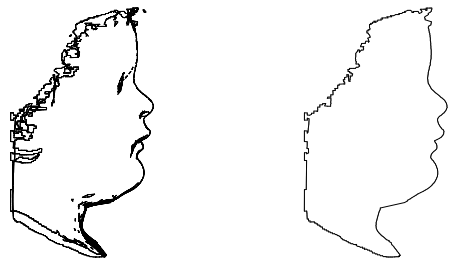

(a) Apparent Contour (b) Boundary

Figure 2: The apparent contour (a) and shadow boundary (b) of a head viewed from the side.

To find the shadow boundary we first calculate the apparent contour [9]. Let $\mathbf{x} = (x, y, z) \in \mathbf{R}^3$ be a point on the surface with normal $\mathbf{n}$ and let $\mathbf{l}$ be the direction of the light rays. If $\mathbf{l} \cdot \mathbf{n} = 0$ then $\mathbf{x}$ is said to lie on the *apparent contour*. In other words $\mathbf{x}$ is on the apparent contour if one of the light rays parallel to $\mathbf{l}$ is tangent to the surface at $\mathbf{x}$. Calculating the apparent contour is a local problem which just needs a test on the adjacent vertices; the surface normals do not need to be calculated and the apparent contour can be calculated in linear time.

Once the points on the apparent contour for $\mathbf{l} = (0, 0, 1)$ have been found we parallel project them onto $z = 0$ by the mapping $\pi : (x, y, z) \to (x, y, 0)$. The resultant set, Figure 2a, consists of the shadow boundary plus some other structure. The boundary, figure 2b, can be easily extracted from this data. Calculating the apparent contour beforehand greatly reduces the time taken to calculate the boundary. Our method retains the exact locations of points on the profile which would be lost if pixel-based mathematical morphology techniques were used.

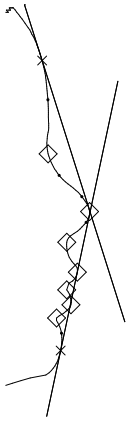

Figure 3: The landmarks used, $\times$ indicates bi-tangent landmarks, $\diamond$ indicates first-stage landmarks and $\bullet$ indicate second-stage landmarks. The two bi-tangent lines are also shown.

4 Finding Landmarks

To calculate a set of landmarks on the profile a hierarchical scheme based on bi-tangents and distances from lines is used.

First the bi-tangent lines connecting the forehead and nose, and the nose and chin are found. The four points of bi-tangency are connected by three line segments. For each segment we then find those points on the profile which are local extremals of distances from the line (both maxima and minima). This strategy gives us points at the top, bottom and tip of the nose, points on the top and bottom lips, a point between the lips and one between the lower lip and chin. We call these *first-stage landmarks*. We then consider the line joining successive bi-tangent points and first-stage landmarks and find the points which are furthest away from these lines. We call these *second-stage landmarks* and they gives us more detail for the forehead and nose. Finally we thin out some of the artificial extrema by hand to get a set common to all subjects. This set is shown in figure 3 and consists of 14 landmarks.

Whilst the points of bi-tangency can be sensitive to slight changes in the profile the subsequent points are more stable. If $\delta\theta$ is the error in the angle of the bi-tangent and κ is the curvature at our landmark, then the error in position is approximately $\frac{1}{\kappa}\delta\theta$. As our first-stage landmarks tend to be near points of high curvature, we see that errors in positions will be small. Furthermore the errors in the angles of lines joining the first-stage landmarks will typically be much less than $\delta\theta$, so we also expect good accuracy for second-stage landmarks.

Calculating landmarks in this way is independent of the orientation of the head; thus our method does not require a notion of "upright", a concept which we have found to be quite subjective.

Our method also avoids the problems associated with calculating curvature-based landmarks (inflections and local extremals of curvature (vertices)). One method for finding these landmarks would be to fit a B spline in two dimensions, smooth it by a Gaussian kernel, calculate the curvature and its derivative and look for zero crossing of each which would give us inflections and vertices respectively. The position and number of such landmarks would be dependent on the amount of smoothing applied, and high levels of smoothing would be required to get a consistent set of landmarks for all individuals. When the profile contains nearly straight or nearly circular segments, as can sometimes be found in the nose and nasal regions, the value of curvature is almost constant, and finding consistent curvature-based landmarks becomes harder. Campos [2] has tackled some of these problems by working in scale space.

Our method of finding landmarks should extend to three dimensions. Instead of working with bi-tangent lines, tri-tangent planes could be used. Finding maximally distant points will, however, present some problems as the maximally distant point will not always lie under the triangle of tri-tangent points.

5 Analysing Growth

Once we have a set of landmarks we can use Generalised Procrustes Analysis and Principal Component Analysis to look at the changes in *size and shape* of the profile as the subjects

age. Here *shape* is defined as all the geometrical information about an object when location, scale and rotational effects are filtered out. First we use Procrustes Analysis to factor out the size, translation and rotation components. This gives a set of tangent space coordinates representing shape. We then add in the size again and perform Principal Component Analysis to pick out the changes in size and shape.

The two-dimensional structure of the profiles allows us to get a representation of average shape by solving a complex eigenvalue problem [10]. For higher dimensions other techniques need to be used. Let $\{\mathbf{z}_i = (z_{i1}, \ldots, z_{ik}) \in \mathbf{C}^k : 1 \leq i \leq m\}$ be a set of m configurations representing m profiles. The components of $\mathbf{z}_i$ are the positions of the k landmarks on the i-th profile expressed as complex numbers. Here $k = 14$. Let the *centre* of $\mathbf{z}_i$ be $\bar{z}_i = \frac{1}{k}\sum_{j=1}^{k} z_{ij} \in \mathbf{C}$ and the *size*, s_i be given by $s_i^2 = \frac{1}{k}\sum_{j=1}^{k} |z_{ij} - \bar{z}_i|^2$. Now let $\mathbf{w}_i = (w_{i1}, \ldots, w_{ik}) \in \mathbf{C}^k$ be the centred, rescaled version of $\mathbf{z}_i$, with $w_{ij} = (z_{ij} - \bar{z}_i)/s_i$. The $\mathbf{w}_i$ represents the shape plus orientation of our profiles. Let $T = \sum_{i=i}^{m} \mathbf{w}_i \mathbf{w}_i^*$, denote a complex covariance matrix ($\mathbf{w}^*$ is the transpose of the complex conjugate of $\mathbf{w}$). This has a dominant eigenvector $\hat{\boldsymbol{\mu}} \in \mathbf{C}^k$ which represents the mean shape of all the profiles. This is independent of orientations in $\mathbf{R}^2$ of the individual profiles. The deviation in shape of each profile from the mean is represented by the Procrustes tangent coordinates:

$$\mathbf{v}_i = e^{-i\theta_i}(I - \hat{\boldsymbol{\mu}}\hat{\boldsymbol{\mu}}^*)\mathbf{w}_i,$$

where $\theta_i = \arg(\hat{\boldsymbol{\mu}}^* \mathbf{w}_i)$. Although $\mathbf{v}_i$ is a k-dimensional complex vector, linear constraints mean that it lies in a $(2k-4)$-dimensional real plane. Define the *shape and size tangent coordinates* for each profile by $\mathbf{u}_i = (\mathrm{Re}(\mathbf{v}_i), \mathrm{Im}(\mathbf{v}_i), \log(s_i)) \in \mathbf{R}^{2k+1}$. These lie in a $2k-3$ dimensional plane.

We perform (real) Principal Component Analysis on the shape and size tangent coordinates $\{\mathbf{u}_i\}$, to find the most important variations in the shape and size of the profiles.

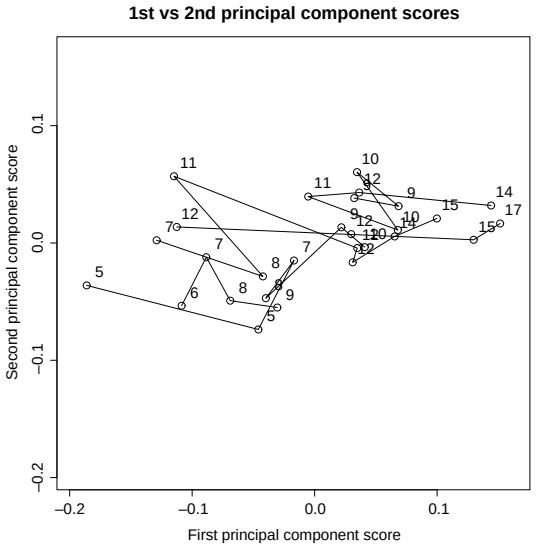

Figure 4: The first and second principal component scores for five subjects at various ages.

The tangent coordinates are grouped by subject and the within group covariance matrix calculated. The eigenvectors of this matrix are used as the basis for the Principal Component Analysis. In practice we found there was little difference between using within-group riance matrix and the full covariance matrix. The first principal component (PC) was found to account for 75 percent of the total variability. Figure 4 shows the first and second principal component scores for each profile. The lines connect the different profiles for the same person at successive ages, and the number by each point is the age. In all there are five subjects with 3, 4, 6, 7 and 8 scans respectively. Notice how the first PC score tends to increases with age. This is graphically illustrated in Figure 5 which shows the first principal component score plotted against age. There is a strong correlation of 0.78 between age and the first PC score. In a few places the first PC score decreases with age. This effect is caused by a variety of factors: the subject pursing the lips on one day and not on the other; artifacts adding by the scanning process and errors in calculating the medial plane and landmarks.

Figure 6 shows the first mode of variation, with the mean profile in the middle, and the ± 3 standard deviations shifted to the left and

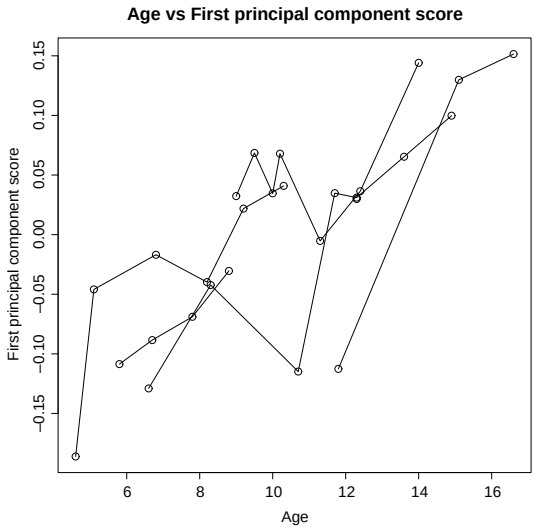

Figure 5: The age of a subject plotted against the first principal component scores.

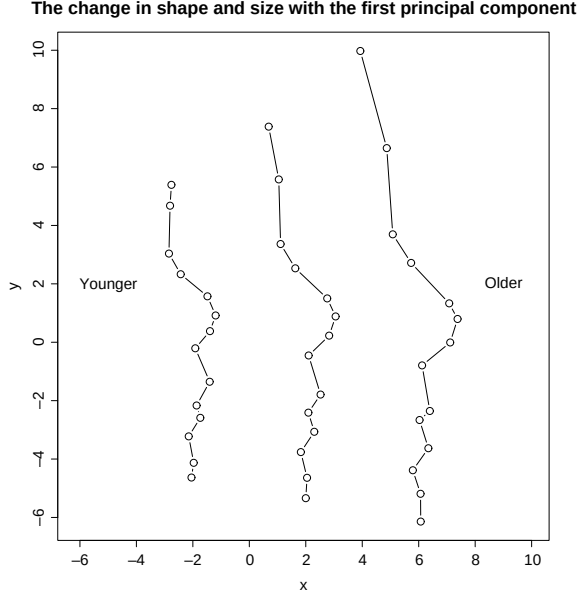

Figure 6: The first mode of variation (± 3 sd). For clarity the three profiles have be shifted along the x-axis.

right The most important change is seen in size, but there is also some change in shape as well. In particular the nose becomes proportionately larger with age and the bridge of the nose lengthens. The nasion region at the top of the nose also becomes less curved with age. There is little change around the mouth, and a slight drop in the chin with age. The forehead appears to slope back with age, but this may be an artifact caused by the point of bi-tangency shifting as the nose grows. Apart from the changes in the forehead, these findings confirm the observations made by anatomists mentioned in the introduction.

6 Conclusions

We have discussed a way for representing the size and shape of the profile of the human face and a method for analysing its growth. The results show that a large proportion of the change in size and shape with growth can be explained by the first principal component. Further, our interpretations are also consistent with those of anatomists. We intend to extend this work to look at the full 3D shape of the face. All the algorithms discussed should generalise to three dimensions.

Our current model has so far only looked at a simple one-dimensional model of growth. Further work is needed to take account of the differences between male and female faces, the differences between the major facial types, and the variations, with age, in the rates of growth of different parts of the face. In particular there is a need for better methods for the quantification of shape change.

More work is needed in the landmark identification. The points found are sensitive to errors in the scanning process and biological variability. These errors can lead to less than optimal registration, and errors in the PCA.

7 Acknowledgements

We are grateful to EPSRC for a grant to carry out this work. We would also like to thank Fred Bookstein for helpful comments.

References

[1] P. J. Besl and N. D. McKay. A Method for Registration of 3-D Shapes. *IEEE Transactions on Pattern Analysis and Machine Intelligence*, 14(2):239–255, Febuary 1992.

[2] J. C. Campos, A. D. Linney, and J. P. Moss. The analysis of facial profiles using scale space techniques. *Pattern Recognition*, 26(6):819–824, 1993.

[3] I. L. Dryden and K. V. Mardia. *Statistical Shape Analysis*. Wiley, 1998.

[4] D. H. Enlow and M. G. Hans. *Essentials of Facial Growth*. Saunders, Philadelphia, 1996.

[5] L. G. Farkas, J. C. Posnick, and T. M. Hreczko. Growth and development of regional units in the head and face based on anthropometric measurements. *Cleft Palate-Craniofacial Journal*, 29:301–302, 1992.

[6] S. A. Feik and J. E. Glover. Growth of children's faces. In J. G. Clement and D. L. Ranson, editors, *Craniofacial Identification in Forensic Medicine*, pages 203–224. Arnold, 1998.

[7] F. Galton. Classification of portraits. *Nature*, 76:617–618, 1907.

[8] F. Galton. Numeralised profiles for classification and recognition. *Nature*, 83:127–130, 1910.

[9] P. J. Giblin. Apparent contours: an outline. *Phil. Trans. Royal Society London, A*, 356:1087–1102, 1998.

[10] J. T. Kent. The complex Bingham distribution and shape analysis. *Journal of the Royal Statistical Society, Series B*, 56(2):285–299, 1994.

[11] K. V. Mardia, F. L. Bookstein, and I. J. Moreton. Statistical assessment of bilateral symmetry of shape. *Biometrika, to appear*, 1999.

[12] J. P. Moss, A. D. Linney, S. R. Grindrod, and C. A. Moss. A laser scanning system for the measurement of facial surface morphology. *Optics and Lasers in Engineering*, 10:179–90, 1989.

[13] C. A. Pelizzari, G. T. Y. Chen, D. R. Spelbring, R. R. Wechselbaum, and C-T. Chen. Accurate three-dimensional registration of CT, PET, and/or MR images of the brain. *J. Computer Assisted Tomography*, 13:20–26, 1989.